Can 25-cp Polymer Solution Efficiently Displace 1,600-cp Oil During Polymer Flooding?

R. S. Seright, New Mexico Institute of Mining and Technology; **Dongmei Wang,** University of North Dakota; and **Nolan Lerner, Anh Nguyen, Jason Sabid,** and **Ron Tochor,** Cona Resources Limited

Summary

This paper examines oil displacement as a function of polymer-solution viscosity during laboratory studies in support of a polymer flood in Canada's Cactus Lake Reservoir. When displacing 1,610-cp crude oil from field cores (at 27°C and 1 ft/D), oil-recovery efficiency increased with polymer-solution viscosity up to 25 cp (7.3 seconds^{-1}). No significant benefit was noted from injecting polymer solutions more viscous than 25 cp. Much of this paper explores why this result occurred. Floods in field cores examined relative permeability for different saturation histories, including native state, cleaned/water-saturated first, and cleaned/oil-saturated first. In addition to the field cores and crude oil, studies were performed using hydrophobic (oil-wet) polyethylene cores and refined oils with viscosities ranging from 2.9 to 1,000 cp. In field cores, relative permeability to water (k_{rw}) remained low, less than 0.03 for most corefloods. After extended polymer flooding to water saturations up to 0.865, k_{rw} values were less than 0.04 for six of seven corefloods. Relative permeability to oil remained reasonably high (greater than 0.05) for most of the flooding process. These observations help explain why 25-cp polymer solutions were effective in recovering 1,610-cp oil. The low relative permeability to water allowed a 25-cp polymer solution to provide a nearly favorable mobility ratio. At a given water saturation, k_{rw} values for 1,000-cp crude oil were approximately 10 times lower than for 1,000-cp refined oil. In contrast to results found for the Daqing polymer flood (Wang et al. 2000, 2011), no evidence was found in our application that high-molecular-weight (MW) hydrolyzed polyacrylamide (HPAM) solutions mobilized trapped residual oil. The results are discussed in light of ideas expressed in recent publications. The relevance of the results to field applications is also examined. Although 25-cp polymer solutions were effective in displacing oil during our corefloods, the choice of polymer viscosity for a field application must consider reservoir heterogeneity and the risk of channeling in a reservoir.

Introduction

The concentration and viscosity of the polymer used in a polymer flood are of critical importance. On the one hand, use of too much polymer can jeopardize the economics of a flood. On the other hand, use of insufficient polymer can promote channeling/viscous fingering and the problems associated with early polymer breakthrough. In several field polymer floods in Canada, 15- to 30-cp polymer solutions were injected to displace 1,000- to 3,000-cp oil (Wassmuth et al. 2009; Liu et al. 2012; Delamaide et al. 2014; Saboorian-Jooybari et al. 2015). Waterflooding has also been applied in a number of cases (Kumar et al. 2008; Beliveau 2009). Controversy exists regarding whether improved results might be seen if greater polymer viscosities were injected. A number of arguments have been offered on both sides of this discussion (Seright 2017). Arguments that have been made in favor of using low polymer viscosities include the following:

1. The relative permeability to water may be surprisingly low.
2. The mobility ratio at the oil/water shock front is much lower than the endpoint mobility ratio.
3. Economics favor using low polymer viscosities.
4. High polymer resistance factors and residual resistance factors reduce the need for high polymer viscosities and volumes.
5. High-viscosity polymer solutions unreasonably impair injectivity.
6. Polymers can emulsify oil in situ, leading to higher-than-expected resistance factors (Vittoratos and Kovscek 2017).

Seright (2017) argued that Reasons 2 through 5 are not generally valid. Concerning Reason 2, the mobility ratio at the shock front was shown not to correlate well with displacement efficiency. Rebutting Reason 3, up to a definable point, higher polymer concentrations are economically favored because solution viscosity increases roughly with the square of polymer concentration; the value of the oil produced relative to the cost of polymer injected is fairly insensitive to polymer concentration; the cost of surface facilities for producing high polymer concentrations is not greatly more than for producing low polymer concentrations; and efficiently displacing oil with a moderate-to-high polymer viscosity delays polymer breakthrough and the accompanying problems. Concerning Reason 4, in moderate- to high-permeability rock, resistance factors (effective polymer viscosity in porous media) that are more than twice the viscosity or residual resistance factors (permeability-reduction values) greater than two are usually laboratory artifacts that will not materialize deep in a reservoir (Seright et al. 2011). Regarding Reason 5, polymers are often injected above the formation-parting pressure, so injectivity need not be a limitation as long as the fractures do not extend too far (Seright et al. 2009; Seright 2017). Reasons 1 and 6 will be discussed further in this paper.

Wang et al. (2000, 2001a, 2001b, 2010, 2011) advocated injecting very viscous high-MW polymer solutions to reduce the residual (capillary-trapped) oil saturation below that expected from prolonged waterflooding. A number of authors performed laboratory investigations of this phenomenon, often using fluid velocities that were significantly higher than those found in the bulk of most reservoirs (Urbissinova et al. 2010; Vermolen et al. 2014; Clarke et al. 2016; Reichenbach-Klinke et al. 2016; Koh et al. 2017). A study by Koh et al. (2017) indicated that at low velocities, the endpoint residual oil saturation was the same for waterflooding and polymer flooding. Erincik et al. (2017) reported experiments (performed at relatively high velocities) where unusually low residual oil saturations were attained by injecting high-salinity polymer solutions after low-salinity polymer solutions.

This paper examines oil displacement as a function of polymer-solution viscosity during laboratory studies in support of a polymer flood in the Cactus Lake Reservoir in Canada. A key result is that 25-cp polymer solutions appeared optimal for displacement of

This paper (SPE 190321) was accepted for presentation at the SPE Improved Oil Recovery Conference, Tulsa, 14–18 April 2018, and revised for publication. Original manuscript received for review 10 January 2018. Revised manuscript received for review 22 April 2018. Paper peer approved 24 April 2018.

1,610-cp crude oil during corefloods. Much of this paper explores why this result occurred. Was it caused by the core, the oil, the saturation history, the relative permeability characteristics, emulsification, or simply the nature of the test? The results are discussed in light of ideas expressed in recent publications. The relevance of the results to field applications is also examined.

Cactus Lake Geological Overview

The Cactus Lake property is in west-central Saskatchewan in Townships 35 and 36, Ranges 27 and 28 W3M, approximately 40 miles south of Lloydminster, Saskatchewan, Canada. Cactus Lake is a heavy-oil property that has been under waterflood since 1988. The largest reservoir in the property produces from the Devonian-Mississippian Bakken Formation and is generally commingled with the Lower Cretaceous Rex Sand. A polymer flood has been under development since 2012, after an extensive vertical-drilling program that transitioned the pool from a 40-acre waterflood to a 10-acre polymer flood. At Cactus Lake, heavy oil is produced from the Mississippian Bakken and Cretaceous Rex Sandstones. The Rex is in partial-to-full communication with the underlying Bakken through the sub-Cretaceous unconformity and is typically commingled for production with the Bakken.

Bakken. The Lower Mississippian Middle Bakken Formation was deposited in a marine shelf environment and later reworked into a series of northeast/southwest-trending sand ridges. The Bakken Formation has three distinct members. The upper and lower members are black organic-rich shales ranging from 3 to 5 m in thickness. The Middle Bakken is typically a very-fine- to fine-grained quartzose sandstone with minor amounts of feldspar, clay, and calcite cement. It is commonly unconsolidated, although the base of the sandstone can contain shaley, cemented, nonreservoir sediments. The middle member reaches a maximum thickness of 30 m. Within the Bakken, porosities average 30% with permeabilities up to 5.0 darcies. Water saturations average 37%. Maximum pay thickness is 33 m, while the average pay thickness is 12 m. The area has a relatively gentle southwest regional dip that has been modified by numerous Torquay collapse features. Pre-Cretaceous erosion has eroded to the base of the overlying Lodgepole carbonate and commonly into the Bakken sandstone. Oil is trapped both structurally and stratigraphically in the preserved Bakken sandstone.

Rex. The Lower Cretaceous Rex Formation was deposited in a deltaic to upper-shoreface marine environment. The Rex sandstone directly overlies the sub-Cretaceous unconformity over most of the pool area and is usually separated from the Bakken by a thin 1- to 4-m layer of shaley detrital deposits. In some areas, the two sands are in direct communication. The Rex pinches out rapidly to the NW (depositional) and SE (onlap) margins. The Rex sandstone is typically a very-fine- to fine-grained quartzose sandstone that exhibits a coarsening-upward profile on logs. It is commonly unconsolidated with porosities averaging 30% and permeabilities up to 5.0 darcies. Water saturations average 30%. Maximum sandstone thickness is 6.5 m, while average pay thickness across the pool is 2.7 m. The area has a relatively gentle SW regional dip, and oil is trapped stratigraphically.

Experimental

Fluids. In this work, synthetic Cactus Lake brine contained 17,269 ppm sodium chloride, 114 ppm potassium chloride, 642.4 ppm $CaCl_2$-$2H_2O$, and 919.9 ppm $MgCl_2$-$6H_2O$ [1.9% total dissolved solids (TDS)]. Two HPAM polymers were used: SNF Flopaam™ 3630S (copolymer with MW of approximately 18 million g/mol and 30% degree of hydrolysis) and SNF Flopaam™ 6030S (post-hydrolyzed with MW of approximately 21 million g/mol and 30% degree of hydrolysis). The structure of the polymers can be found in Green and Willhite (1998). Polymers were selected by the operator based on commercial considerations. Polymer solutions were prepared using brine that was filtered through 0.45-μm Millipore filters. The HPAM polymer solutions were prepared by the standard vortex-mixing method. The polymer solutions were not filtered after preparation. At 7.3 seconds^{-1} shear rate in synthetic Cactus Lake brine at the reservoir temperature of 27°C using 3630S HPAM, 5-cp viscosity (μ_p) was achieved with 725 ppm polymer, 25-cp viscosity with 1,900 ppm polymer, 50-cp viscosity with 2,690 ppm polymer, and 203-cp viscosity with 5,250 ppm polymer. Using 6030S HPAM, 6-cp viscosity was achieved with 650 ppm polymer, 25-cp viscosity with 1,650 ppm polymer, and 52-cp viscosity with 2,350 ppm polymer. Plots of viscosity vs. shear rate for the polymer solutions (at 27°C) are presented in **Fig. 1.** Viscosities were determined using an Anton Paar MCR 301 rheometer with CC27-SN29031 and a measuring system with $d = 0$ mm (concentric cylinder).

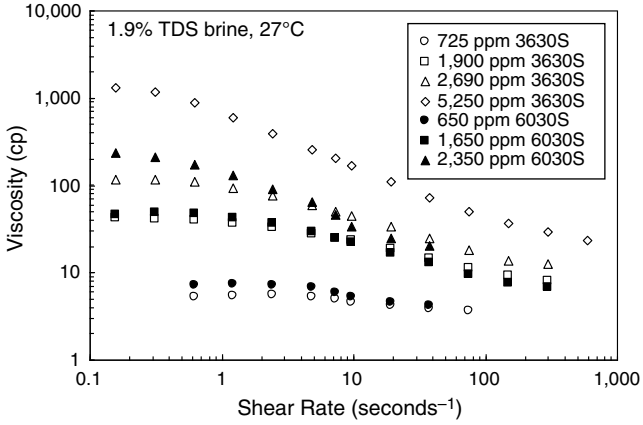

Fig. 1—Viscosity vs. shear rate for polymer solutions.

At 27°C, Cactus Lake crude-oil viscosity ranged from 990 to 1,610 cp, depending on the particular sample. For the field core experiments described in **Tables 1 and 2** (except Core 1), the oil viscosity was 1,610 cp. For the remaining experiments (in Core 1 and the porous polyethylene cores), the crude-oil viscosity was 1,000 cp. The oil was Newtonian in behavior (viscosity was independent of shear rate). For experiments later in this paper, clear, paraffinic, Newtonian refined oils were used, with a range of viscosities. Properties of these oils are listed in **Table 3.** Interfacial tensions (IFTs) were measured against synthetic Cactus Lake brine using the pendant-drop

method (with a DataPhysics Contact Angle System OCA). All refined oils could pass through a 0.45-μm filter (Millipore) without plugging. Cactus Lake crude oil passed readily through a 5-μm filter without plugging, but not through a 2-μm filter.

Polymer viscosity at 7.3 seconds^{-1} and 27°C	1	5.2	25.1	50.5	203
Polymer	–	3630	3630	3630	3630
Polymer concentration (ppm)	0	725	1,900	2,690	5,250
Core number	1	24	27	26	29
Core length (cm)	6.12	6.43	6.11	6.41	6.61
Core diameter (cm)	3.81	3.81	3.81	3.81	3.81
PV (cm^3)	24.5	24.89	23.5	24.5	25.8
Porosity	0.352	0.339	0.338	0.335	0.343
Permeability to oil (md)	690*	1,142	1,100	1,635	991
Water breakthrough (PV)	0.02	0.059	0.070	0.128	0.107
% of OOIP from 1.5 PV of water	27.4	29.8	30.5	39.1	43.7
Added % of OOIP after 1.5 PV of polymer	–	28.7	28.8	28.5	25.7
Added % of OOIP after 3 PV of polymer	–	39.1	47.1	38.0	33.7
Final % of OOIP after polymer	–	72.9	80.1	85.6	82.6
% of OOIP for polymer over 1.5 PV of water	–	43.1	49.6	46.5	38.9
Added % of OOIP after 40 PV of brine	–	3.0	3.3	0.9	1.4
Final Oil Saturation (S_o)	0.301	0.218	0.166	0.135	0.146
Estimated Water Saturation (S_{wr})	0.22	0.109	~0	~0	0.095

*Absolute permeability to water was 976 md.

Table 1—Reservoir-core/flood properties for HPAM with MW = 18 million g/mol. OOIP = original oil in place.

Polymer viscosity at 7.3 seconds^{-1} and 27°C	1	6.1	25.0	52.2
Polymer	–	6030	6030	6030
Polymer concentration (ppm)	0	650	1,650	2,350
Core number	23	20	30	21
Core length (cm)	5.736	6.700	6.593	6.477
Core diameter (cm)	3.81	3.81	3.81	3.81
PV (cm^3)	21.99	24.72	24.50	25.24
Porosity	0.336	0.324	0.326	0.342
Permeability to oil (md)	410	206	229	310
Water breakthrough (PV)	0.056	0.155	0.071	0.145
% of OOIP from 1.5 PV of water	15.9	17.2	20.7	18.8
Added % of OOIP after 1.5 PV of polymer	–	22.5	25.0	23.3
Added % of OOIP after 3 PV of polymer	–	30.0	31.6	30.2
Final % of OOIP after polymer	–	55.9	63.4	56.3
% of OOIP for polymer over 1.5 PV of water	–	38.7	42.7	37.5
Added % of OOIP after 40 PV of brine	–	0.5	1.2	2.0
Final Oil Saturation (S_o)	0.478	0.387	0.314	0.363
Estimated Water Saturation (S_{wr})	0.141	0.099	0.113	0.091

Table 2—Reservoir-core/flood properties for HPAM with MW = 21 million g/mol. OOIP = original oil in place.

Cores and Flooding Procedures. Cactus Lake field cores were 3.81 cm in diameter and 11.40 cm^2 in the cross-sectional area. The core length averaged 6.5 cm, the porosity averaged 0.33, and the pore volume (PV) averaged 24.5 cm^3. Details of the cores and flooding results can be found in Tables 1 and 2. As received (i.e., with the resident oil/water in place), the cores were mounted horizontally in a biaxial Hassler sleeve and an overburden pressure of 1,500 psi was applied for the duration of the coreflood. A fixed temperature of 27°C was maintained by circulating water from a temperature bath through tubing that was wrapped around the Hassler cell. Crude oil in the amount of 100 cm^3 (approximately 4 PV) was forced through the core at a flux (Darcy velocity) of 1 ft/D (14.48 cm^3/h) using a

Model 500D Isco pump. This pump measures pumped fluid by volume and is accurate to 0.01 cm^3. For cores flooded with a copolymerized HPAM with 18×10^6 g/mol MW and 30% degree of hydrolysis (3630S in **Fig. 2**), permeability to oil at connate-water saturation averaged 1,220 md. For cores flooded with a post-hydrolyzed HPAM with 21×10^6 g/mol MW and 30% degree of hydrolysis (6030S in **Fig. 3**), permeability to oil at connate-water saturation averaged 250 md.

Oil	Viscosity (cp)	Density (g/cm^3)	Oil/Brine IFT (mN/m)
Cactus Lake crude	990 to 1,610	0.960	7.43
Cannon S600	1,000	0.843	24.3
Equate mineral oil	130	0.840	22.9
Cannon S20	28	0.855	17.9
Soltrol 170	2.9	0.779	13.2

Table 3—Properties (at 27°C) of oils used.

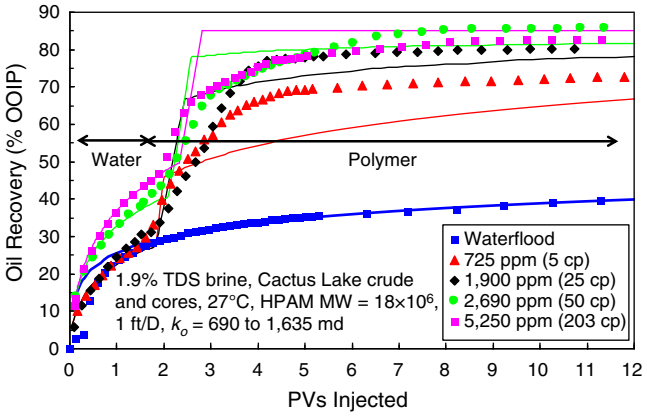

Fig. 2—Oil-recovery response in high-permeability field cores.

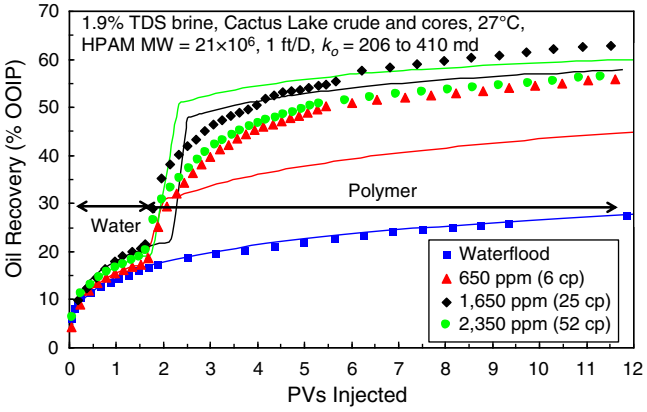

Fig. 3—Oil-recovery response in less-permeable field cores.

After oil saturation, approximately 1.5 PV of synthetic Cactus Lake brine was injected at 1 ft/D. Relative permeability to water and to oil was calculated using continuously monitored pressure across the core, oil production, and water cut. Oil/water separations were accomplished by centrifugation and oil adherence to polyethylene sample tubes. After 1.5 PV of brine, water cuts were more than 90% for all cores. In seven cores, approximately 10.5 PV of the polymer solution was injected, followed by approximately 40 PV of the brine. Subsequently, approximately 40 PV of toluene and 40 PV of methanol were injected to clean the core. Finally, the core was dried in an oven to remove the solvents. Mass balances were used to estimate residual oil saturation (S_o) at a given stage of the experiment and to estimate the initial water saturation in the core (S_{wi}).

A dilemma exists when coreflooding with viscous oils, regarding whether to flood at high or low rates. By flooding at high rates, the capillary end effect can be minimized if the cores are water-wet (Willhite 1986). In contrast, Maini (1998) proposed the use of low flooding velocities when measuring relative permeability with viscous oils to minimize complications associated with fines migration and in-situ emulsification. According to Maini (1998), low flooding velocities are also more representative of fluid velocities in the bulk of the reservoir. Another major concern with using high rates is mobilization of residual oil and attainment of relative permeability values that would not be achievable at typical reservoir rates. This work will demonstrate that this concern is justified for our cases **(Figs. 4 and 5).** A third point is that high fluid velocities could accentuate viscous fingering in water-wet cores (Peters and Flock 1981; Doorwar and Mohanty 2017). Mai and Kantzas (2010) noted that although capillary forces are typically thought to be negligible in heavy-oil reservoirs, they can be important and can result in significant oil recovery. Consequently, a low rate (1-ft/D Darcy velocity)

was chosen for our corefloods. Although measurements might be distorted by the capillary end effect near the time of water breakthrough, our interest in relative permeability is focused on measurements made well after water breakthrough. Experiments were performed with various wetting states of the field cores (native, water-saturated first, oil-saturated first) in hopes of assessing how strongly the capillary forces affected our results. Further, studies were performed in strongly oil-wet porous polyethylene cores for comparison.

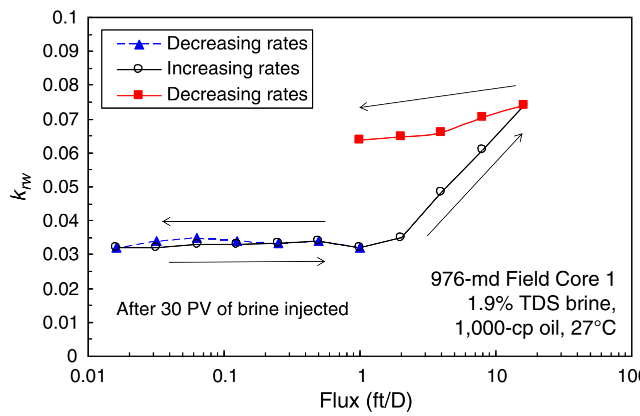

Fig. 4—Effect of injection flux on k_{rw} in Field Core 1 after 30 PV.

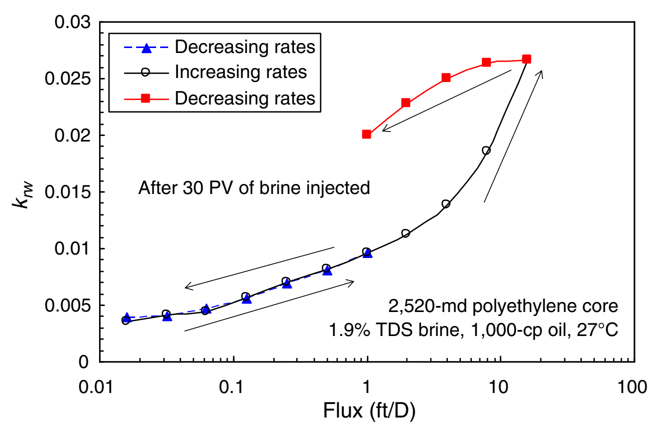

Fig. 5—Effect of injection flux on k_{rw} in a polyethylene core after 30 PV.

Results

25-cp Polymer Solution Appears Optimal for Oil Displacement in Corefloods. Oil recovery vs. PVs injected is plotted in Figs. 2 and 3 for the two HPAM polymers. Tables 1 and 2 provide additional details for the cores and floods. Fig. 2 and Table 1 apply to HPAM with MW = 18 million g/mol in 690- to 1,635-md cores; Fig. 3 and Table 2 apply to HPAM with MW = 21 million g/mol in 206- to 410-md cores. (The lower-MW polymer used high-permeability cores simply because those experiments were performed first, and the best cores were used at that time. Later, when the higher-MW polymer was tested, only less-permeable field cores were available.)

For a given condition, oil recovery was consistently greater in the high-permeability cores (Fig. 2) than in the less-permeable cores (Fig. 3). Waterflood responses in the four less-permeable cores (Fig. 3) were quite similar, with oil-recovery values ranging from 15.9 to 20.7% original oil in place (OOIP) after 1.5 PV of water injection. For three of the more-permeable cores (blue, red, and black data in Fig. 2), waterflood responses were also similar, with oil-recovery values ranging from 27.4 to 30.5% OOIP after 1.5 PV of water injection. However, two of the more-permeable cores showed noticeably higher recovery values (39.1 and 43.7% OOIP) after 1.5 PV of waterflooding (green circles and pink squares in Fig. 2).

Each of the waterflood data sets (i.e., the first 1.5 PV in Figs. 2 and 3) were fitted to Brooks-Corey equations:

$$k_{rw} = k_{rwo}[(S_w - S_{wi})/(1 - S_{or} - S_{wi})]^{nw}, \quad (1)$$

$$k_{ro} = [(1 - S_w - S_{or})/(1 - S_{or} - S_{wi})]^{no}, \quad (2)$$

where k_{rw} is relative permeability to water, k_{ro} is relative permeability to oil, S_w is water saturation, S_{wi} is initial water saturation, S_{or} is residual oil saturation, and superscripts *nw* and *no* are saturation exponents. (In this work, the endpoint relative permeability to oil is assumed to be unity, depending on oil permeability at S_{wi}.) Parameters from the fits are listed in **Table 4.** These values were used as input into fractional-flow calculations (Seright 2010) to project oil recovery during subsequent polymer injection. No gravity, capillary pressure, retention, or inaccessible-PV effects were included in these calculations. Details of the assumptions associated with the calculations can be found in Seright (2010) and in the associated spreadsheets on our website at http://baervan.nmt.edu/groups/res-sweep/. In Figs. 2 and 3, each solid curve of a given color is the fractional-flow projection associated with the data of that same color. Note that more than one set of parameters might provide an adequate fit. For example, waterflooding of Core 1 (first row of Table 4) lists fitting

parameters of $S_{wi} = 0.17$, $S_{or} = 0.35$, $k_{rwo} = 0.05$, $nw = 2$, and $no = 3$. An acceptable alternative fit could be obtained using $S_{wi} = 0.1$, $S_{or} = 0.15$, $k_{rwo} = 0.7$, $nw = 3.5$, and $no = 4$. Because multiple fits could be obtained to a given curve, fixed values for S_{wi} and S_{or} were typically chosen (for a given set of core permeabilities) in hopes of making the recovery curves as comparable as practically possible.

	Core	Fluid	k_{rwo}	S_{wi}	S_{or}	nw	no
High-permeability cores	1	Water	0.05	0.17	0.35	2	3
	24	5-cp 3630	0.12	0.1	0.15	1.5	2
	27	25-cp 3630	0.12	0.1	0.15	1.5	2
	26	50-cp 3630	0.035	0.1	0.15	1.5	2.2
	29	200-cp 3630	0.035	0.1	0.15	1.5	1
Low-permeability cores	23	Water	0.6	0.15	0.3	2	3
	20	6-cp 6030	0.6	0.15	0.3	2	2
	30	25-cp 6030	0.35	0.15	0.3	2	2
	21	52-cp 6030	0.45	0.15	0.3	2	2

Table 4—Fractional-flow fitting parameters for Figs. 2 and 3.

After injecting 1.5 PV of brine, approximately 10.5 PV of polymer solution was injected. This volume of polymer was chosen to provide a high probability that the core was swept near residual oil saturation by the end of the flooding process. Of course, we recognize that 10.5 PV will not be injected in a field application. For both polymers, a substantial increase in oil recovery was noted when switching from water to polymer injection (data points in Figs. 2 and 3). In the more-permeable cores (Fig. 2), fractional-flow projections predicted that oil recovery should increase with increased viscosity of the injected polymer; however, relatively modest differences were projected near the end of polymer injection. The data indicated that the highest ultimate recovery was from the 50-cp polymer solution, although ultimate recoveries for the 25-, 50-, and 203-cp-polymer solutions were not greatly different. Interestingly, the incremental recovery (over the recovery noted at 1.5 PV of waterflooding) was highest for the 25-cp-polymer solution (fourth-to-last row in Table 1).

In the less-permeable cores (Fig. 3) after injecting approximately 10.5 PV of polymer solution, the 25-cp polymer solution (black diamonds) provided the highest oil recovery. Oil recovery when injecting 52-cp polymer solution (green circles) was comparable with that when injecting 6-cp polymer solution. The fractional-flow projection for 52-cp polymer solution (green curve in Fig. 3) was modestly higher than for the 25-cp polymer solution (black curve).

No Reduction of S_{or}. The previously discussed observations (especially the fourth-to-last rows in Tables 1 and 2) indicate maximum oil recovery associated with injecting 25-cp polymer solution. One could argue that recoveries for the 25- to 203-cp-polymer-solution cases were similar (for a given core permeability) and that differences were simply because of core-to-core variations or experimental error. Nonetheless, for this particular oil and set of cores, high concentrations of high-MW HPAM polymers did not convincingly drive the residual olil saturation below expectations from prolonged waterflooding. This result is in opposition to that observed for the Daqing polymer flood (Wang et al. 2000, 2001a, b, 2010, 2011), where concentrated high-MW polymers reportedly drove the residual olil saturation down by 15 saturation-percentage points. In Fig. 2, actual ultimate oil recoveries were slightly greater than projections for the 25- and 50-cp polymer solutions but slightly less than projections for the 203-cp polymer solution. In Fig. 3, actual ultimate oil recoveries were greater than projections for the 25-cp but less than projections for the 50-cp polymer solution.

Other observations are relevant to the current literature discussion on the effects of polymer concentration and viscosity on the displacement of trapped residual oil. Because our experiments used a fixed injection rate of 1 ft/D, the capillary number when injecting 25-, 50-, and 203-cp polymer solutions should be 25 to 203 times higher when injecting polymer than for the previous water injection (because rate and IFT were constant). Consequently, the displacement of additional oil was expected with increased polymer concentration. Evidence of mobilization of residual oil is presented later (Figs. 4 and 5) when waterflood flux increased from 1 to 16 ft/D. Because oil recovery did not increase noticeably for polymer concentrations greater than 25 cp (Figs. 2 and 3), the HPAM polymer solutions apparently did not mobilize trapped residual oil for our floods. Also, note in the second-to-last rows in Tables 1 and 2, significant volumes of residual oil were recovered by toluene extraction at the end of the experiments. The literature observations of polymers mobilizing trapped residual oil in other applications (e.g., Daqing) are not doubted here. Our work only indicates that polymers do not mobilize trapped residual oil in our application. For many previous reports where polymer flooding apparently reduces the endpoint S_{or}, it is noteworthy that injection rates and capillary numbers were relatively high.

Additional insight into the apparent optimum associated with 25-cp polymer solutions might come from **Fig. 6.** Fig. 6 replots the oil-recovery projections using the parameters in Table 4. However, instead of plotting oil recovery in % of OOIP (as in Figs. 2 and 3), Fig. 6 plots the percentage of mobile oil recovered. When presented in this way, Fig. 6 shows that (except at low PV) recovery projections bunch together (more than 90% of mobile oil recovered) for polymer viscosities of 25 cp and greater. This observation implies that the apparent "optimum" of 25-cp polymer solution noted in Figs. 2 and 3 simply reflects core-to-core variations in endpoint water and oil saturations. Put another way, if the reservoir was homogeneous with linear flow, little incremental oil would be recovered by injecting polymer solution greater than 25 cp. The consequences if the reservoir is not homogeneous will be discussed later.

Anomaly With 5- to 6-cp Polymer Solutions. Interestingly, in both Figs. 2 and 3, the fractional-flow projections for the 5- to 6-cp polymer solutions (red curves) were notably below the actual polymer data points (red triangles). Vittoratos and Kovscek (2017) speculated that emulsification might be the dominant mechanism for polymer flooding of viscous oils, rather than viscosity increase. They speculate that above some minimum concentration (e.g., 3 cp), polymers might promote the formation of viscous emulsions that improve the mobility ratio and provide a "self-diversion" mechanism. In the present work, the oil/water effluent did not appear to be significantly emulsified, either by water or polymer injection. For the cases tested, the aqueous effluent was not more viscous than the injected water or polymer solution. Further, the viscosity of the produced oil was the same as that for the injected oil. On the other hand, one could use the 5- to 6-cp-HPAM-solution data as possible support for the emulsification idea. Fractional-flow calculations were performed to assess the "effective polymer viscosity" required to match the observed oil-recovery values in Figs. 2 and 3. In

Fig. 2, matching the data for the 5-cp HPAM solution (red triangles) required an assumption of 10-cp polymer solution during the fractional-flow calculations. Matching the data for the 25-cp HPAM solution (black diamonds in Fig. 2) required an assumption of 40-cp polymer solution. However, if in-situ emulsification was truly responsible for the increased apparent viscosity, it appeared to be a modest effect (i.e., a factor of two or less). The emulsification concept might appear stronger when viewing the data in the less-permeable core (Fig. 3). Matching the data for the 6-cp HPAM solution (red triangles) required an assumption of 29-cp polymer solution, while matching the data for 25-cp HPAM solution (black triangles) required an assumption of 80-cp polymer solution. The results in the less-permeable cores indicate a viscosity enhancement of three- to six-fold, in contrast to the 1.6- to twofold enhancement in the more-permeable cores. If the emulsification concept is valid, this result argues against a "self-diversion" mechanism because the "emulsion" apparently restricted less-permeable flow paths more than high-permeability flow paths. If a process (e.g., emulsion formation) restricts flow in less-permeable paths by a greater factor than in high-permeability paths, sweep efficiency will be reduced. Further insights into this topic can be found in Seright (1988) and Seright and Liang (1995). Additional thoughts on emulsions and their possible role in polymer flooding can be found in Vittoratos and Kovscek (2017).

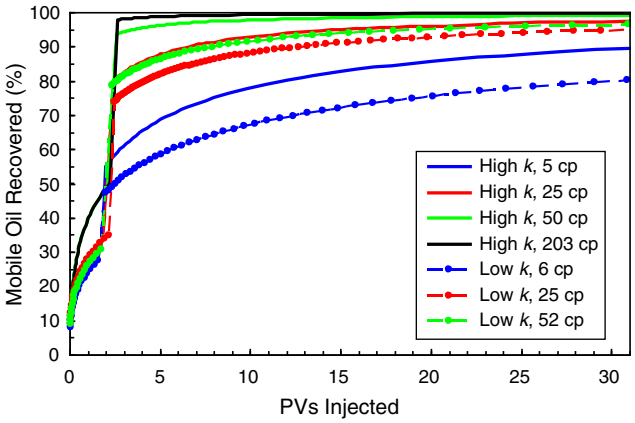

Fig. 6—Replot of fractional-flow projections from Table 4: percentage of mobile oil recovered vs. PV.

Two other ideas will be discussed later to explain the discrepancy between the 5- to 6-cp recovery data and the fractional-flow projections. One concept, derived from the work of Doorwar and Mohanty (2017), involves reduced viscous fingering to improve recovery more than would be expected from fractional-flow calculations. The second concept is that the resistance factors for the polymer solutions were significantly greater than the expectations from the viscosity measurements.

Relative Permeabilities for Field Cores. Calculations of relative permeability were made using the method of Johnson et al. (1959), as modified by Jones and Roszelle (1978). For the field cores mentioned previously, during water injection, **Figs. 7 and 8** plot the relative permeability to water and oil, respectively. In both Figs. 7 and 8, the solid symbols (including the asterisk) refer to the high-permeability cores and the open symbols refer to the less-permeable cores. The key result from Fig. 7 is that relative permeability to water remained low, less than 0.03 for water saturations up to 0.42. Further, relative permeability to oil remained reasonably high (greater than 0.05) for most of this range (Fig. 8). These observations help explain why only 25-cp polymer solutions were effective in recovering 1,610-cp oil. The low relative permeability to water (<0.03) allowed the 25-cp polymer solution to provide a nearly favorable mobility ratio. At the same time, the relatively high relative permeability to oil (> 0.05) allowed oil behind the water front to continue flowing at a reasonable rate.

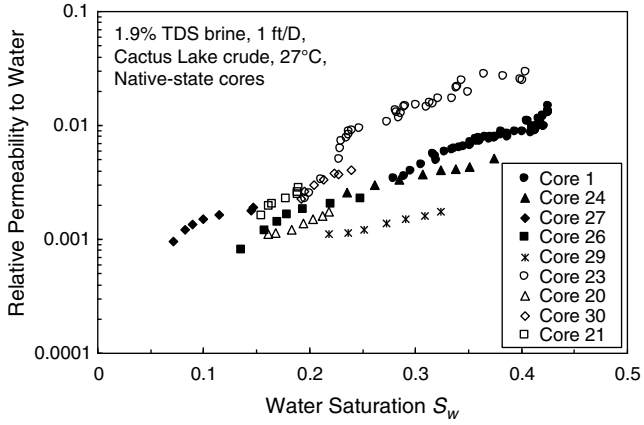

Fig. 7—Relative permeability to water for field cores.

Because the highest water saturation achieved in Fig. 7 was 0.42, a substantial amount of mobile oil remained after waterflooding. Thus, the relative permeability to water might be expected to rise substantially after polymer flooding drives a given core to a higher water saturation. To examine this possibility, **Table 5** lists the k_{rw} values calculated after injecting 10.5 PV of polymer solution into

seven of the cores from Fig. 7. The third and fourth columns in Table 5 list S_w and k_{rw} values after 1.5 PV of water injection, and the fifth and sixth columns list S_w and k_{rw} values after a subsequent 10.5 PV of polymer injection. The top four listings apply to the most-permeable (approximately 1 darcy) cores, while the bottom three listings apply to the less-permeable (approximately 250 md) cores. As mentioned previously, the k_{rw} values for waterflooding were calculated by the methods of Johnson et al. (1959) and Jones and Roszelle (1978). For a given polymer flood, k_{rw} values at the end of 10.5 PV of polymer injection were estimated by

$$k_{rw(\text{after 10.5 PV of polymer})} = [k_{rw}(\Delta p/\mu_w)]_{(\text{after 1.5 PV of water})} \times (\mu_p/\Delta p)_{(\text{after 10.5 PV of polymer})}, \quad (3)$$

where Δp is the pressure drop across the core, measured at a fixed rate of 1 ft/D. The non-Newtonian character of polymer solutions complicates the estimation of k_{rw} values. In this case, polymer-solution viscosity (μ_p) in Eq. 3 was taken as the value at 7.3 seconds^{-1} (as listed in the second column of Table 5). (The possible error associated with this assumption can be judged by examining the rheological curves in Fig. 1. The error is likely to be greatest for the 203-cp solution because of its greater shear-thinning character.) After 10.5 PV of polymer injection, S_w values were approximately 0.85 in the high-permeability cores and approximately 0.65 in the less-permeable cores (fifth column of Table 5). Interestingly, the final k_{rw} values (last column of Table 5) were less than 0.04 in six of the seven cases. (The exception was the 203-cp-polymer-solution case, where the greatest error might be associated with the in-situ viscosity estimate.) Thus, the k_{rw} values generally remained low even after extensive polymer flooding to achieve high water saturations (i.e., low oil saturations). The question persists of exactly why k_{rw} values should remain so low at high water saturations. To offer some speculation, we noted that the Cactus Lake oil can pass through a 5-μm filter but not through a 2-μm filter. Perhaps some hydrophobic particulate (e.g., asphaltene) coats the rock. In the vicinity of pore throats, this adsorbed hydrophobic particulate might aid in restricting water flow while providing a film pathway that enhances oil flow.

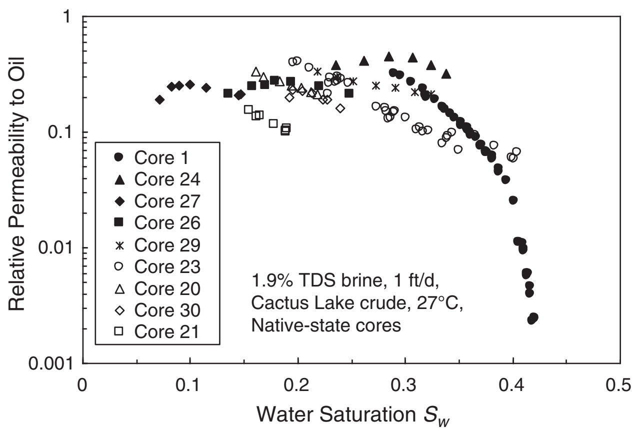

Fig. 8—Relative permeability to oil for field cores.

		After 1.5 PV of Water		After 10.5 PV of Polymer	
Core *k* (md)	Polymer (cp)	S_w	k_{rw}	S_w	k_{rw}
1,142	5	0.375	0.0051	0.782	0.0094
1,100	25	0.147	0.0019	0.834	0.0175
1,635	50	0.248	0.0023	0.865	0.0366
991	203	0.324	0.0017	0.854	0.0931
206	6	0.218	0.0017	0.613	0.0038
229	25	0.223	0.0038	0.686	0.0123
310	52	0.190	0.0029	0.637	0.0211

Table 5—k_{rw} values after polymer flooding.

Maini (1998) reviewed the challenges associated with measuring relative permeability for heavy-oil reservoirs. He noted that damage to cores can affect relative permeabilities, especially because debris or permeability reductions on core faces can have a substantial effect. In our cases, we hoped to minimize this effect by inspection of core faces and use of filtered fluids. However, the possibility of core damage cannot be excluded. It is possible that this effect can explain some of the differences in relative permeability curves seen in Figs. 7 and 8.

Maini (1998) and Huh and Pope (2008) noted that core heterogeneity can accentuate viscous fingering/channeling through cores that affect recovery efficiency and consequently the measurements of relative permeability. For two cases (Field Core 1 and Polyethylene Core 1), tracer studies were performed on cleaned, oil-free cores, using the method described in Seright and Martin (1993). In both cases, tracer-breakout curves were very sharp with no tailing, indicating homogeneous cores.

When calculating relative permeability in Figs. 7 and 8, capillary pressure was neglected. Maini (1998) discussed the problems with this assumption. Because our experiments were conducted at a low rate, capillary pressure effects might have distorted the relative permeability values near the time of water breakthrough, if the cores were water-wet. This concern will be addressed after by performing experiments with different sequences of core saturation and by using cores that are strongly oil-wet. Also, as mentioned previously, our primary interest in relative permeability focuses on the time well after water breakthrough.

Effects of Saturation History, Oil, and Oil Viscosity. A key result from the previous studies was that injection of 25-cp polymer solution appeared optimal for displacement of 1,610-cp oil from the field cores. Was this result because of the saturation history, the nature of the oil, or the oil viscosity?

Field Core 1 was subjected to extended (30 PV) water injection during additional studies of saturation history and the nature of oil used for saturation. In the first experiment, the core was received in its native state, saturated with crude oil, and flooded with brine, just as with the other field cores mentioned previously (except that 30 PV of brine was injected in Field Core 1). After 30 PV of brine injection, the core was flushed with 40 PV of toluene, followed by 40 PV of methanol to clean the core. Then the core was dried. For the second experiment, the cleaned core was saturated with brine, followed by saturation with crude oil, and then 30 PV of brine, and then it was cleaned as in the first experiment. The third experiment was identical to the second, except that the core was first saturated with oil instead of brine. The fourth experiment was identical to the second, except that the oil was Soltrol 170, a refined oil with a viscosity of 2.9 cp at 27°C. The fifth experiment was identical to the second, except that the oil was Cannon S600, a refined oil with a viscosity of 1,000 cp at 27°C.

During the course of injecting 30 PV of brine, **Figs. 9, 10, and 11** plot oil recovery, relative permeability to water, and relative permeability to oil, respectively. **Table 6** lists relative permeability fitting parameters associated with the curves in Fig. 9. As expected, oil recovery was very efficient when brine displaced 2.9-cp oil, relative permeability to water rapidly approached the endpoint value of 0.24, and relative permeability to oil rapidly dropped to low values (seen in Figs. 9, 10, and 11, respectively). Also as expected, displacement efficiency was substantially lower for the 1,000-cp oils than for the 2.9-cp oil. Fig. 9 shows that displacement of 1,000-cp oil was most efficient for the refined S600 oil (black diamonds) in the cleaned core and least efficient for the crude oil in the native-state core (red circles). Displacement efficiencies were similar for the cleaned cores that were first saturated with water (blue triangles in Fig. 9) and that were first saturated with crude oil (green squares). For the various cases using 1,000-cp oils, relative permeability to oil showed considerable scatter and similar behavior within the experimental error (Fig. 11). (The data scatter for k_{ro} occurred because oil drops were produced erratically at high water cuts.)

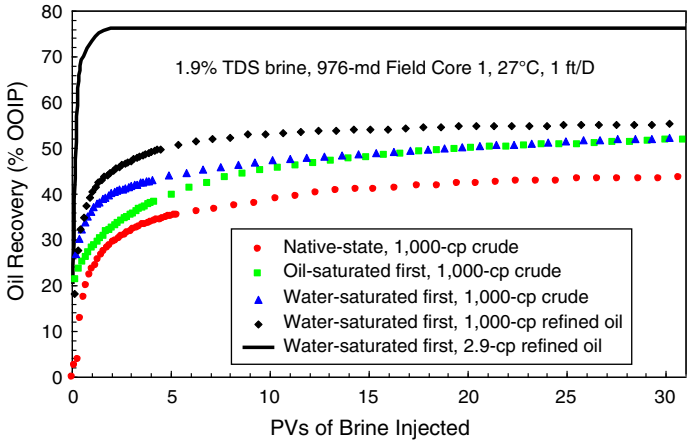

Fig. 9—Oil recovery vs. PV for Core 1.

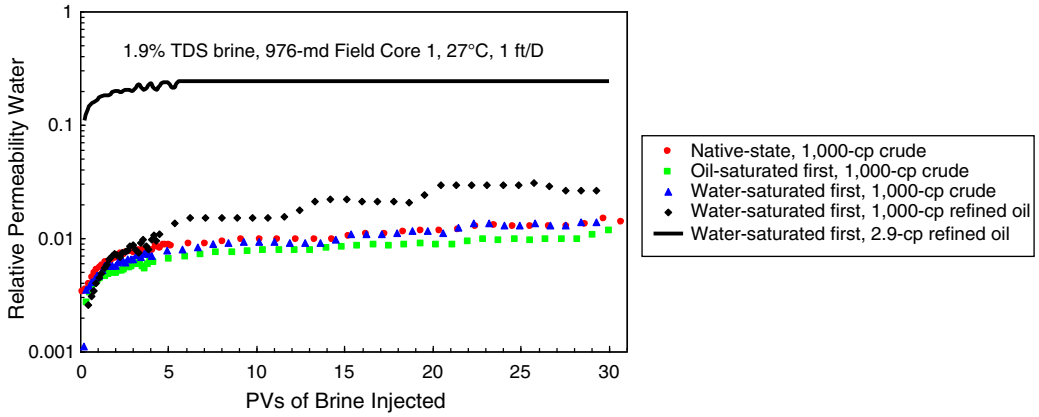

Fig. 10—Relative permeability to water vs. PV for Field Core 1.

Fig. 9 demonstrates that oil recovery was inefficient for all four cases involving water displacement of 1,000-cp oil. The relative permeability to water was low after 30 PV of brine injection, ranging from 0.014 to 0.035 for the 1,000-cp-oil cases. In examining the fits to the oil-recovery curves (Fig. 9 and Table 6), the assumed endpoint k_{rwo} values were not unusually low (0.05 to 0.09). Thus, although the saturation history and oil nature (refined vs. crude) can affect displacement efficiency, their effects do not substantially alter the inefficient nature of water displacing 1,000-cp oil.

For Field Core 1, **Figs. 12 and 13** plot relative permeability to water and oil, respectively, vs. water saturation. Relative permeability to water showed similar shapes and trends for all four cases with 1,000-cp oil, including the 1,000-cp refined oil (black diamonds in Fig. 12). However, the k_{rw} curves shifted with water saturation. The k_{rw} curve associated with the native-state core (perhaps the most

oil-wet) was shifted most toward low water saturations, whereas the curve associated with the 1,000-cp refined oil (probably the most water-wet) was shifted most to high water saturations. The k_{rw} curve for the 2.9-cp refined oil (red triangles in Fig. 12) could be viewed as an extension of the trend associated with the 1,000-cp oils. As with the other field cores (Fig. 7), values for k_{rw} remained less than 0.03 for much of the testing (up to water saturations of 0.63 for 1,000-cp refined oil).

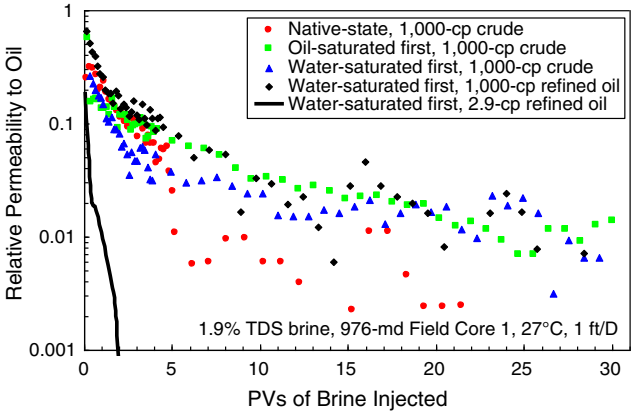

Fig. 11—Relative permeability to oil vs. PV for Field Core 1.

Saturation History	Oil	Oil Viscosity (cp)	k_{rwo}	S_{wi}	S_{or}	nw	no
Native state	Crude	1,000	0.05	0.17	0.35	2	3
Water first	Crude	1,000	0.09	0.1	0.15	2.3	4
Oil first	Crude	1,000	0.09	0.1	0.15	2.3	4
Water first	Cannon S600	1,000	0.05	0.1	0.15	4.4	5
Water first	Soltrol 170	2.9	0.24	0.1	0.2	1.5	1.7

Table 6—Fractional-flow fitting parameters for Fig. 9 (Field Core 1).

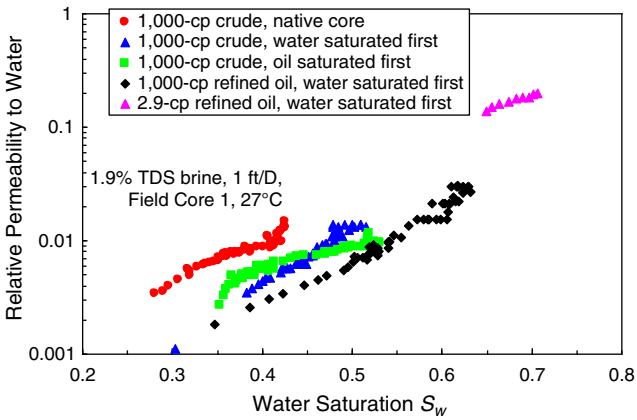

Fig. 12—Relative permeability to water vs. S_w for Field Core 1.

In Fig. 13, relative permeability to oil exhibited similar shapes and trends for all five oils. Again, the curves showed significant shifts with water saturation. The three crude-oil k_{ro} curves were somewhat close together, whereas the two refined-oil k_{ro} curves were shifted to higher water saturations. In all five cases, k_{ro} remained greater than 0.05 for a significant range of saturation, just as was noted for Fig. 8.

Behavior in Porous Polyethylene Cores. The field cores used in the preceding sections contained approximately 85% quartz or feldspars, 10% iron oxide, and 2.5% clay (mostly kaolinite). This subsection describes corefloods in porous polyethylene cores. These cores are described in Seright et al. (2006) and have a pore structure (pore-size distribution, pore-throat distribution) that is similar to Berea sandstone. However, grain surfaces are quite smooth, in contrast to the rough appearance of clays on quartz grains (Seright et al. 2006). As expected, the porous polyethylene cores were strongly hydrophobic and exhibited very high contact angles with all oils tested (i.e., those in Table 3).

Five waterfloods were performed in a single porous polyethylene core using five different oils (Table 3). The brine was the same as that used in the other parts of this work (1.9% TDS). Only waterfloods (not polymer floods) were performed here. The core was 3.81 cm in diameter and 6.27 cm long, with a porosity of 0.305, absolute permeability of 2,000 md, and PV of 21.8 cm^3. As with the previous cores, the experiments were performed at 27°C and an injection flux of 1 ft/D. The overburden pressure was 200 psi because

the core could be crushed and reduced in porosity with high confining pressures. In the first experiment, the core was saturated with brine, flooded with 4 PV of 2.9-cp Soltrol 170 oil, and then flooded with 30 PV of brine. The core was then flooded with 4 PV of 28-cp Cannon S20 oil in preparation for the second experiment, where 30 PV of brine was injected. This procedure was repeated using 130-cp Equate mineral oil for the third experiment, 1,000-cp Cannon S600 oil for the fourth experiment, and 1,000-cp Cactus Lake crude for the fifth experiment. Results are shown in **Figs. 14 through 16.** The cores were not cleaned between experiments because we felt that the refined oils and the clean polyethylene cores would allow an efficient saturation of the core when a viscous oil displaced a less-viscous oil.

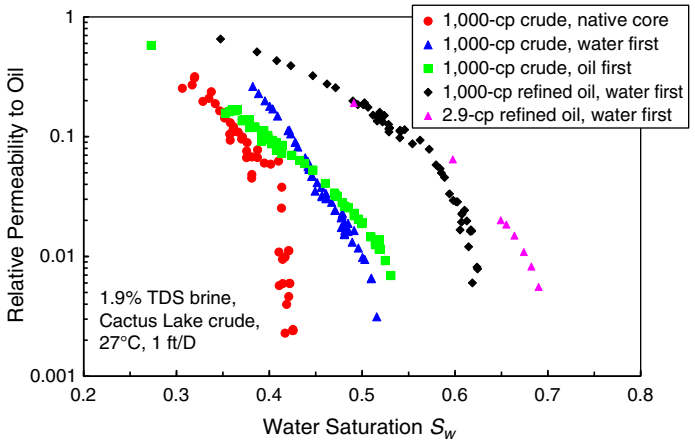

Fig. 13—Relative permeability to oil vs. S_w for Field Core 1.

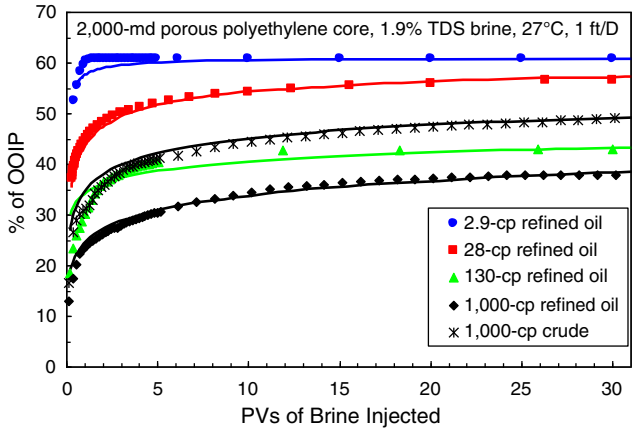

Fig. 14—Oil recovery during water injection in a polyethylene core vs. oil viscosity.

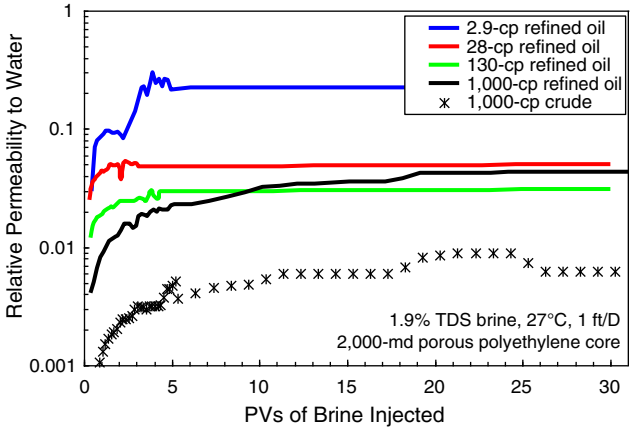

Fig. 15—k_{rw} in a polyethylene core during water injection vs. oil viscosity.

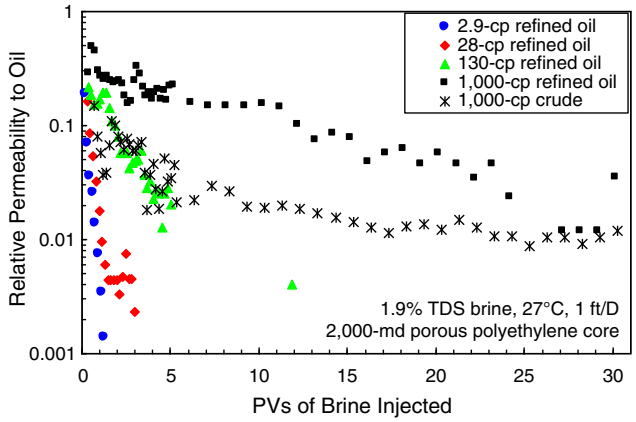

Fig. 16—k_{ro} in a polyethylene core vs. oil viscosity.

Fig. 14 shows the waterflood-recovery efficiency for the five oils. The data points of a given color show the actual recovery values at a given PV, whereas the solid curves of that color show the fit to Eqs. 1 and 2 using the parameters in **Table 7.** For the refined oils, a good fit was obtained for all refined oils using $S_{wi} = 0.18$, $S_{or} = 0.32$, $k_{rwo} = 0.24$, and $k_{roo} = 1$. For the crude oil, a much-lower k_{rwo} value (0.02) was needed. For the refined oils, at a given brine PV throughput, oil recovery decreased with increased oil viscosity, as expected. However, surprisingly, oil recovery with the 1,000-cp crude oil was higher than expected, exceeding that for the 130-cp mineral oil.

Oil	Oil Viscosity (cp)	k_{rwo}	S_{wi}	S_{or}	nw	no
Soltrol 170	2.9	0.24	0.18	0.32	4	2
Cannon S20	28	0.24	0.18	0.32	2.7	2.5
Equate mineral oil	130	0.24	0.18	0.32	5.5	5.5
Cannon S600	1,000	0.24	0.18	0.32	3.4	3.4
Crude	1,000	0.02	0.18	0.32	3	3.5

Table 7—Fractional-flow fitting parameters for Fig. 14 (Polyethylene Core 1).

Fig. 15 plots relative permeability to water for the five oils. At a given PV, relative permeability to water was quite high (approximately 0.24) for the refined 2.9-cp oil. For the 28-, 130-, and 1,000-cp refined oils, the relative permeabilities to water after 10 PV of brine were similar, in the range from 0.02 to 0.04. Interestingly, k_{rw} values associated with the 1,000-cp crude oil were 3 to 10 times lower than for the 28- to 1,000-cp refined oils. This effect appears to be responsible for crude-oil recovery being higher than oil recovery associated with the 130-cp oil (Fig. 14).

Fig. 16 plots relative permeability to oil for the five oils. Interestingly, the curve for the 1,000-cp crude was more similar to that for the 130-cp mineral oil than for the 1,000-cp refined oil. The case with 1,000-cp refined oil maintained the highest k_{ro} values for the highest PV throughputs.

Figs. 17 and 18 plot relative permeability vs. water saturation. The refined oils exhibited similar k_{rw} and k_{ro} behavior. Although modest deviations were noted (especially for the 2.9-cp refined oil), the relative permeabilities (for both k_{rw} and k_{ro}) followed approximately the same behavior for all four refined oils (with viscosities of 2.9, 28, 130, and 1,000 cp). Relative permeability to oil (Fig. 18) for the 1,000-cp crude oil was also similar to that for the refined oils. In contrast, the relative permeability to water for the crude oil (Fig. 17) was approximately 10 times lower than for the refined oils (for a given water saturation). As mentioned previously, the lowest k_{rw} values for the 1,000-cp crude oil explain the relatively high recovery seen in Fig. 14.

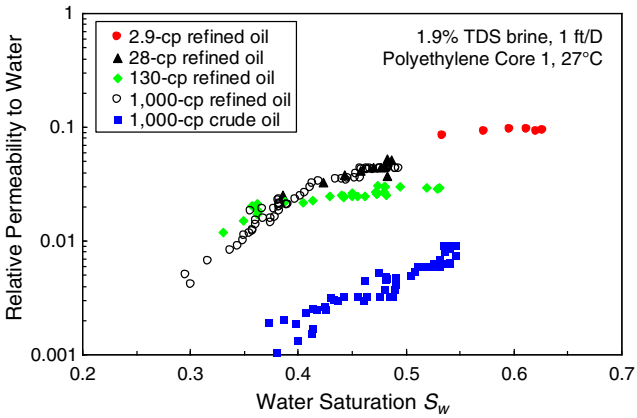

Fig. 17—k_{rw} in a polyethylene core vs. water saturation.

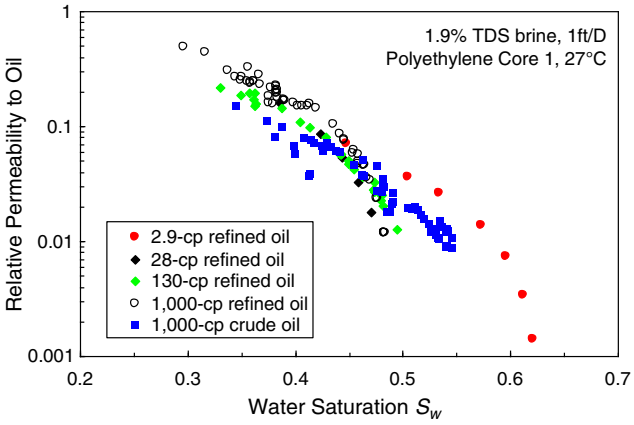

Fig. 18—k_{ro} in a polyethylene core vs. water saturation.

Previous literature is qualitatively consistent with our observations. With a few exceptions, much of the literature indicates that relative permeability behavior is not sensitive to oil viscosity, although it is sensitive to wetting behavior (Willhite 1986). Sandberg et al. (1958) found that relative permeability to oil or water was not affected by oil viscosity (for refined oils) between 0.398 and 1.683 cp in 4- to 6-in.-long sandstone cores. In 1-ft-long 325/200-mesh sandpacks, Richardson (1957) found that the ratio of k_{rw}/k_{ro} was the same for 1.8-cp kerosene and 151-cp oil (of unspecified origin). Odeh (1959) presented a controversial paper in which he noted that the apparent relative permeability to oil increased dramatically with increased oil viscosity at relatively low water saturations. However, at higher water saturations, his relative permeabilities appeared more in line with Willhite (1986) (i.e., not sensitive to oil viscosity). Wang et al. (2006) studied crude oils with viscosities ranging from 430 to 13,550 cp in 5.6-in.-long, 1.67-in. diameter, 100/60-mesh Ottowa sandpacks. They reported that relative permeability to both water and oil decreased significantly with increased oil viscosity in the water-saturation range between 40 and 60%. However, a close look at their data revealed that their k_{rw} and k_{ro} values were insensitive to oil viscosity from 430 to 1,860 cp. Substantial differences were seen only for oil viscosities of 5,410 cp and greater.

Effect of Fluid Velocity. For two experiments, after injecting 30 PV of brine to displace 1,000-cp oil, the water-injection rate was varied to examine the effect on the relative permeability to water. One experiment was performed in Field Core 1 (Fig. 4), while the other was performed in a 2,520-md porous polyethylene core (Fig. 5). In both cases, the experiment started with an injection flux of 1 ft/D. After stabilization, the pressure was recorded and k_{rw} was calculated. Then the rate was cut in half, and stabilization was again allowed. This procedure was repeated using successively lower rates, down to a flux of 0.016 ft/D (blue triangles in Figs. 4 and 5). Next, the flux was progressively doubled in stages up to a maximum of 16 ft/D (open circles in Figs. 4 and 5). Finally, the flux was again halved in stages back to a value of 1 ft/D (red squares in Figs. 4 and 5).

In Field Core 1 (Fig. 4), k_{rw} was independent of flux between 1 ft/D and 0.016 ft/D, regardless of whether rates were decreasing or increasing. Because the measurements were made over the course of a relatively small throughput (0.8 PV), no significant changes in water saturation occurred, so a constant k_{rw} was expected. As flux was raised from 2 to 16 ft/D, k_{rw} rose from 0.032 to 0.074. This increase in k_{rw} was attributed to increased oil mobilization associated with raising the capillary number. When the rates were subsequently decreased from 16 to 1 ft/D (red squares), k_{rw} values remained above 0.063, consistent with mobilization and reduction of residual oil. Similar behavior was noted in a porous polyethylene core (Fig. 5), except that a reversible velocity effect was noted on k_{rw} for flux values between 0.016 and 1 ft/D.

Discussion and Relevance To Field Applications

Consistency With Previous Literature. Several researchers reported results of corefloods where polymer solutions displaced heavy oil. Asghari and Nakutnyy (2008) used an unspecified polyacrylamide (concentrations from 500 to 10,000 ppm in 1% TDS brine) to displace either 1,000- or 8400-cp oils from either 2.1- or 13-darcy sandpacks. As expected, oil recovery was significantly higher for flooding packs containing 1,000-cp oil than for packs containing 8,400-cp oil. For a given polymer concentration and oil viscosity, oil recovery was modestly higher as rate decreased from 50 to 1 ft/D, possibly indicating a small reduction in viscous fingering associated with capillary effects in water-wet packs. Surprisingly, they found that oil recovery increased only slightly as polymer concentration was raised from 0 ppm (i.e., waterflooding) to 1,000 ppm. Oil recovery did increase noticeably as polymer concentration increased from 5,000 to 10,000 ppm. Viscosities of the polymer solutions were not specified, but the results suggest that viscosity and polymer MW may have been low compared with current HPAM solutions that are commercially used for polymer flooding. The requirement of at least 5,000 ppm polymer to mobilize significant oil argues against the emulsification mechanism proposed by Vittoratos and Kovscek (2017). If HPAM is sufficiently interfacially active to promote emulsification, one might expect emulsification to occur with much less than 5,000 ppm polymer.

Wang and Dong (2007) studied polymer flooding of homogeneous and "heterogeneous" sandpacks that were saturated with 1,450-cp oil. Results from their studies were qualitatively consistent with conventional expectations for polymer flooding. First, in both homogeneous and heterogeneous sandpacks, oil recovery improved monotonically with increased polymer viscosity (from 2.1 to 76.3 cp). Second, oil recovery was ultimately greater and more efficient in homogeneous packs than in heterogeneous packs.

Beyond these observations, which are consistent with accepted polymer-flooding concepts, a statement was made by Wang and Dong (2007) that could be interpreted differently depending on the reader: "There existed a lower limit and an upper limit of the effective viscosity of polymer solution" (for effectively displacing oil). On the surface, this statement is not necessarily inconsistent with conventional mobility-ratio concepts, as demonstrated by Figs. 7.6 through 7.8 of Craig (1971). If the polymer/oil-mobility ratio is low and the porous medium is homogeneous, a mobility ratio of 0.01 is not any more effective than 0.1 in displacing oil. (Put another way, if all the mobile oil has been displaced, there is little point in injecting more polymer.) At the other end, if the polymer/oil-mobility ratio is high and the reservoir is very heterogeneous, poor sweep efficiency results whether the mobility ratio is 10 or 100. (Of course,

mobility-ratio concepts predict that sweep efficiency would improve eventually if the mobility ratio was reduced to a sufficiently low value.) The data of Wang and Dong (2007) and our data do not support the speculation from Vittoratos and Kovscek (2017) that "the efficacy of polymer flooding is independent of polymer concentration after it exceeds the minimum value needed to support emulsification of water into the oil."

Fabbri et al. (2014) observed that a 70-cp polymer solution was reasonably effective at displacing a 5,500-cp oil, especially when applied after waterflooding. Skauge et al. (2014) and de Loubens et al. (2017) demonstrated the value of fingering patterns developed during waterflooding in aiding viscous-oil displacement during subsequent polymer flooding.

Levitt et al. (2013) performed polymer floods (2 PV at 2 ft/D) in either 2-darcy Bentheimer cores or 5-darcy silica sandpacks, displacing a 2,000-cp oil. Before polymer flooding, at least 5 PV of water was typically injected. As with our current experiments, Levitt et al. (2013) matched the waterflood performance using Eqs. 1 and 2. Using these matches, they found that fractional-flow projections were in rough agreement with the experimental results of a 60-cp-HPAM-solution flood. They also found that a 3-cp HPAM solution was surprisingly effective in displacing oil. (This result is consistent with our findings with 5- to 6-cp polymer solution displacing 1,000-cp oil in Figs. 2 and 3.) Levitt et al. (2013) offered several possible explanations, including adsorbed polymer in throats overcoming capillary pressure necessary to mobilize trapped oil; oil emulsification; induction of elongational shear at the surface of viscous fingering; and reduction of residual oil within the fingers. Levitt et al. (2013) noted that polymer retention can severely restrict the application of low-concentration polymer flooding. Much of their paper focused on stability criteria for viscous fingering. Using a number of published criteria for viscous stability, Levitt et al. (2013) said most previous laboratory corefloods using viscous oils are in the "transition region," where oil recovery is sensitive to core diameter.

Doorwar and Mohanty (2017) Analysis. The analysis of Doorwar and Mohanty (2017) provides an interesting means to view our data. They propose a dimensionless scaling factor, N_I, to predict unstable displacements.

$$N_I = (v_w \mu_w / \sigma)(\mu_o / \mu_w)^2 (D^2 / k), \quad (4)$$

where ν_w is interstitial fluid velocity, μ_w is water viscosity, μ_o is oil viscosity, σ is oil/water IFT, D is core diameter, and k is permeability. Viscous fingering should be more severe as N_I increases. Doorwar and Mohanty (2017) used this parameter to correlate with oil recovery at water breakthrough, as shown in **Fig. 19.** Luo et al. (2017a) applied this approach during reservoir simulations.

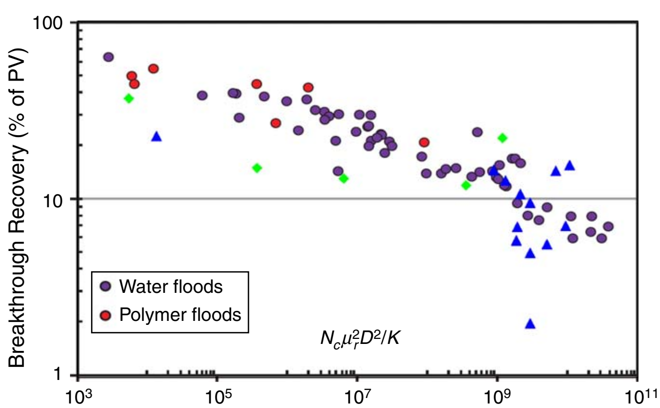

Fig. 19—Plot from Doorwar and Mohanty (2017). Blue triangles are our waterflood data in field cores. Green diamonds are our waterflood data in polyethylene cores.

Some concepts from the development of Eq. 4 [and previous correlations, such as from Peters and Flock (1981)] are that immiscible viscous fingering makes the displacement worse than predicted by Buckley-Leverett analysis (using the "true" Brooks-Corey relations); viscous fingering should be much worse in most field applications (waterflooding heavy oils) than in laboratory corefloods because the porous-medium dimensions (effectively D^2 in Eq. 4) are much larger; and attempts to measure a set of "true" relative permeability curves can be distorted if the porous-medium dimensions (e.g., D^2 in Eq. 4) are too large, if the oil/water-viscosity ratio is too high, and if the velocity is too high and the core is water-wet.

For the waterfloods in Figs. 2 and 3 (in this paper), the Doorwar and Mohanty (2017) N_I (Eq. 4) is between 10^9 and 10^{10}. The blue triangles and green diamonds in Fig. 19 show that water-breakthrough values from our work fall more or less in line with the correlation from Doorwar and Mohanty (2017), although our data from the oil-wet polyethylene cores (green diamonds) generally fall below the water-wet-core data of Doorwar and Mohanty (2017). Doorwar and Mohanty (2017) introduced a model whereby a parameter, λ, characterized the fraction of the cross-sectional flow area that was occupied by a viscous water finger in an oil zone. Therefore, λ ranged from zero to unity. In their model, the "pseudo" or measured relative permeability to water equals λ times the "true" relative permeability to water (i.e., if no viscous fingering occurred). Thus, if significant viscous fingering occurs (as is suggested by the blue triangles in Fig. 19), the measured relative permeability to water is significantly less than the "true" or finger-free value. That concept is qualitatively consistent with the low k_{rw} values in Figs. 7, 12, and 17. The model of Doorwar and Mohanty (2017) also predicts that the "pseudo" or measured relative permeability to oil might be higher than the "true" value because a significant amount of oil flow comes from outside the region of water fingering (where $k_{ro} \approx 1$). That prediction is also qualitatively consistent with our relatively high k_{ro} values in Figs. 8, 13, and 18.

The concepts from Doorwar and Mohanty (2017) may qualitatively help explain why low-viscosity polymer [5- to 6-cp cases in Figs. 2 and 3 and the 3-cp case from Levitt et al. (2013)] provided a better displacement than projected from fractional-flow calculations. The "pseudo" relative permeability curves measured during waterflooding were influenced by viscous fingering, resulting in a lower oil recovery than would be predicted by "true" relative permeability curves. By injecting 5- to 6-cp polymer solution, the N_I parameter was driven to lower values in Fig. 19, resulting in less viscous fingering and normal fractional-flow improvement from

injecting viscous polymer. The combination of both factors makes it appear that oil recovery was higher than expected from fractional-flow projections for polymer flooding (the 5- and 6-cp projections in Figs. 2 and 3).

Continuing the interpretation, the reason that the 25-cp polymer solution recovered as much oil as the 200-cp solution (in displacing 1,000-cp oil in Figs. 2 and 3) was that with the 25-cp polymer solution, no viscous fingering or channeling occurred and the fractional-flow projections were close to "topping out" on oil recovery. (This observation also confirms that the trapped residual olil saturation was not driven below expectations from infinite waterflooding.) However, the observation does not necessarily indicate that 25 cp is the best choice for a field application. The dimensions of the field application (width×height, or the D^2 term in Eq. 4) make viscous fingering much more likely in the field than in the laboratory. Of course, heterogeneity/permeability contrast will also accentuate "fingering" or "channeling." The field applications should require polymer solutions at least as viscous as those required in laboratory corefloods.

The preceding arguments are qualitative. To quantify predictions using the Doorwar and Mohanty (2017) concepts, Luo et al. (2017b) developed an expanded fractional-flow analysis. Their analysis was applied to the 5-cp-polymer-solution flood in Fig. 2 and the 6-cp-polymer-solution flood in Fig. 3. For our cases, predictions made using the analysis of Luo et al. (2017b) (red and black asterisks in **Fig. 20**) were not greatly different from the standard fractional-flow analysis (red and black solid curves in Fig. 20). Thus, an alternative explanation is needed for the observed oil-recovery data in Figs. 2 and 3 for the 5-cp- and 6-cp polymer solutions.

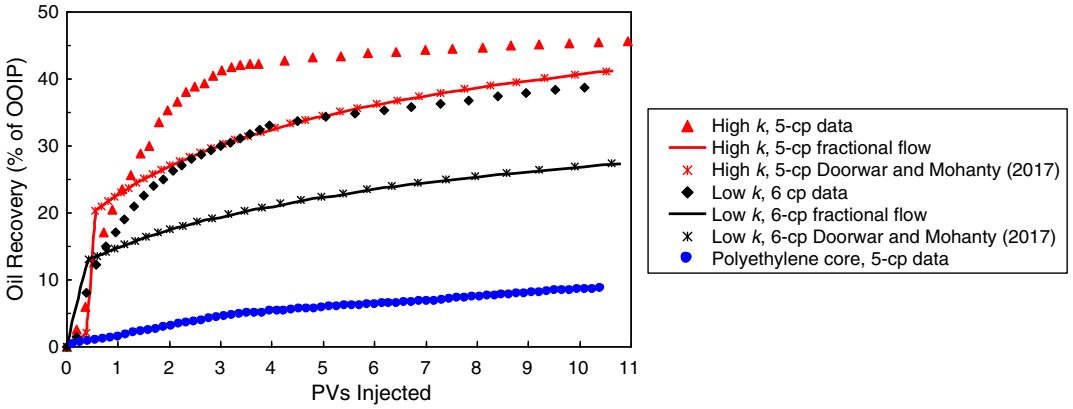

Fig. 20—Oil recovery injecting 5- to 6-cp polymer solution after 1.5 PV of water. Fingering alone does not explain the results.

In-Situ Emulsion Formation. The issue of in-situ emulsion formation was discussed previously. As mentioned, Vittoratos and Kovscek (2017) speculated that emulsification may be the dominant mechanism for polymer flooding of viscous oils, rather than viscosity increase. Although we cannot exclude the possibility that emulsion flow led to higher-than-expected oil recovery for our 5- and 6-cp-polymer solutions (red triangles and curves in Figs. 2 and 3), the emulsification mechanism is not convincing in view of our results. No signs of emulsified oil or water were noted during our experiments. Also, as Maini (1998) noted, emulsification is normally expected at velocities greater than those present in the bulk of most reservoirs. Our experiments were conducted at a low flux of 1 ft/D, which should reduce the probability of in-situ emulsification. To reiterate, an alternative explanation is needed for the observed oil-recovery data in Figs. 2 and 3 for the 5-cp- and 6-cp polymer solutions.

Higher-Than-Expected Resistance Factors. A viable explanation for the observed data is that the resistance factor for the 5-cp polymer solution in Fig. 2 was twice as high as the viscosity would suggest. As noted previously, there was an assumption of 10 cp for the polymer solution for the fractional-flow projections to match the 5-cp-polymer data in Fig. 2. Similarly, as mentioned previously, an assumption of 29 cp for the polymer solution was required for the fractional-flow projections to match the 6-cp-polymer-solution data in Fig. 3, meaning that the resistance factor was approximately five times greater than the viscosity would suggest. This behavior is consistent with previous observations. Seright et al. (2011) noted that freshly prepared HPAM solution can provide resistance factors that are notably greater than viscosities. The high-MW polymer species that causes this effect is destroyed by a modest amount of mechanical degradation or by flow through a short distance of porous rock (Seright et al. 2011). Thus, this resistance-factor effect cannot be expected to penetrate very far into a reservoir. Further, higher-MW HPAMs are more likely to plug (exhibit high resistance factors and residual resistance factors) cores as the permeability decreases, consistent with a 21-million-g/mol polymer providing a resistance factor five times greater than viscosity in 206-md rock, while an 18-million-g/mol polymer provided a resistance factor two times greater than viscosity in 1,142-md rock. Additional studies of this effect can be found in Wang et al. (2008) and Guo (2017).

The most-effective way to confirm this explanation would be to first force a volume of 5- to 6-cp polymer solution through a long field core, as was done in Seright et al. (2011), and then displace crude oil from a separate core. Unfortunately, our supply of field cores was too limited for this approach. As an alternative, a 5-cp-polymer-solution flood was performed in a 2,380-md polyethylene core (after 1.5 PV of waterflood). This approach assumes that HPAM retention will be much lower in the hydrophobic polyethylene core than in the quartzitic field cores, leading to resistance factors and oil-recovery values in the polyethylene cores that are much closer to expectations from the 5-cp-polymer-solution viscosity. The blue circles in Fig. 20 show results from the 5-cp-HPAM-solution flood displacing 1,000-cp crude oil from the 2,380-md polyethylene core. Consistent with the proposed hypothesis, the oil recovery displacement, shown by the blue circles, was considerably less efficient than in the field cores. Also, consistent with expectations, polymer retention in the polyethylene core was substantially lower than in the quartzitic field cores. In the polyethylene core, polymer was detected in the core effluent within 0.13 PV of starting injection of 5-cp HPAM solution. In contrast, for the field cores, polymer was not detected in the effluent until 1 PV of polymer-solution injection.

During flooding of viscous oils, the mobility ratio is critically important not only because of the standard Buckley-Leverett ideas but also because the "stability equations" of Doorwar and Mohanty (2017), as well as Peters and Flock (1981), have the mobility ratio strongly built into them (see Eq. 4).

Relevance To Field Applications. Although 25-cp HPAM solutions effectively displaced 1,000- to 1,610-cp oil during corefloods, 25 cp is not necessarily sufficient for a field application. As noted by Peters and Flock (1981) and Doorwar and Mohanty (2017), the flow area in a field application is tremendously larger than in a coreflood, thus radically accentuating the opportunity for viscous fingering if the mobility ratio is unfavorable. Further, reservoir heterogeneity and the potential for crossflow between layers can greatly accentuate the need for higher polymer viscosities when mobility ratios are unfavorable (Craig 1971; Sorbie and Seright 1992; Seright 2010, 2017).

Previous work (Seright 2010, 2017) indicated that the ideal polymer-solution viscosity for maximizing sweep efficiency in a polymer flood is different for reservoirs with single zones vs. multiple zones and with no crossflow vs. multiple zones with crossflow. If the reservoir can be considered a single zone with uncorrelated permeability variations, then the optimal polymer viscosity would lower the water/oil-mobility ratio to nearly unity. The same polymer viscosity is optimal for reservoirs with multiple zones but no crossflow between zones. In reservoirs with distinct layers and free crossflow between layers, the ideal viscosity is estimated by the product of the water/oil-mobility ratio and the permeability contrast (Seright 2017).

For comparison, a three-injector pilot polymer flood in the Tambaredjo Reservoir in Suriname explored injection of 45- to 125-cp HPAM solutions to displace 600- to 1,700-cp oil (Moe Soe Let et al. 2012; Manichand et al. 2013; Manichand and Seright 2014; Delamaide et al. 2016; Wang et al. 2017). The reservoir description indicated a 12:1 permeability contrast between two flooded zones, revealing potential for significant incremental oil recovery by injecting up to 200-cp polymer solutions (Moe Soe Let et al. 2012; Wang et al. 2017). Interestingly, an analysis of pilot performance by Delamaide et al. (2016) suggested that increasing viscosity beyond 45 cp did not result in any obvious increase in oil recovery. Additional analysis (Wang et al. 2017) indicated that a number of factors could have contributed to this finding, including a high compressibility of the formation; the unconfined nature of the pilot project; staged addition of two additional patterns to the original flood; increases in injected-polymer viscosity during the project; and the condition of the wells (especially damage to production wells).

Conclusions

This paper examines oil displacement as a function of polymer-solution viscosity during laboratory studies in support of a polymer flood in the Cactus Lake Reservoir in Canada.

1. When displacing 1,610-cp crude oil from field cores (at 27°C and 1 ft/D), oil-recovery efficiency increased with polymer-solution viscosity up to 25 cp (7.3 seconds^{-1}). No significant benefit was noted from injecting polymer solutions more viscous than 25 cp.
2. No evidence was found that high-MW HPAM solutions mobilized trapped residual oil in our application.
3. In field cores, relative permeability to water remained low, less than 0.03 for most corefloods. After extended polymer flooding to water saturations up to 0.865, k_{rw} values were less than 0.04 for 6 of 7 corefloods. Relative permeability to oil remained reasonably high (greater than 0.05) for most of the flooding process. These observations help explain why 25-cp polymer solutions were effective in recovering 1,610-cp oil. The low relative permeability to water allowed 25-cp polymer solution to provide close to a favorable mobility ratio.
4. When plotted vs. the percentage of mobile oil recovered, seven polymer floods were consistent with fractional-flow projections in that most of the mobile oil was efficiently recovered by polymer solutions with 25-cp viscosity (or greater).
5. Relative permeability to water showed similar shapes and trends for three cases with 1,000-cp crude oil and one case with 1,000-cp refined oil. Values for k_{rw} remained lower than 0.03 for much of the testing (up to water saturations of 0.63 for 1,000-cp refined oil). Values for k_{ro} remained higher than 0.05 for a significant range of saturation.
6. In a hydrophobic polyethylene core, relative permeability trends were consistent with previous literature in that oil and water relative permeabilities were not sensitive to oil viscosity (from 2.9 to 1,000 cp for refined oils). However, at a given water saturation, relative permeability to water for 1,000-cp crude oil was approximately 10 times lower than for 1,000-cp refined oil.
7. Our results were qualitatively consistent with the concepts developed by Doorwar and Mohanty (2017) in that during waterflooding, apparent k_{rw} values were lower than expected and apparent k_{ro} values were higher than expected if no viscous fingering occurred. However, application of the fractional-flow version of their concept underpredicted oil recovery when using 5- to 6-cp polymer solutions.
8. A viable explanation for the observed data for the 5- to 6-cp polymer solutions is that the resistance factors were two to five times higher than the viscosity suggests. Previous work demonstrated that this effect is a laboratory-scale issue that will not propagate deep into a reservoir.
9. Although 25-cp polymer solutions were effective in displacing oil during our corefloods, the choice of polymer viscosity for a field application must consider reservoir heterogeneity and the enhanced risk of viscous fingering in a reservoir during unfavorable displacements.

Nomenclature

D = core diameter, c.
k = permeability, darcies [μm^2]
k_{ro} = relative permeability to oil
k_{roo} = endpoint relative permeability to oil
k_{rw} = relative permeability to water
k_{rwo} = endpoint relative permeability to water
MW = polymer molecular weight, g/mol
no = oil-saturation exponent in Eq. 2
nw = water-saturation exponent in Eq. 1
N_I = Doorwar and Mohanty (2017) viscous-fingering stability parameter in Eq. 4, dimensionless
OOIP = original oil in place, bbl [m^3]
S_o = oil saturation
S_{or} = residual oil saturation
S_w = water saturation
S_{wi} = initial water saturation
v_w = flux, ft/D [m/d]
Δp = pressure difference, psi [Pa]

λ = Doorwar and Mohanty (2017) viscous-fingering parameter
μ_o = viscosity of oil, cp [mPa·s]
μ_p = viscosity of polymer, cp [mPa·s]
μ_w = viscosity of water, cp [mPa·s]
σ = interfacial tension, mN/m
ϕ = porosity

Acknowledgments

Thanks to Tianguang Fan for measuring IFTs and contact angles. The guidance of Alice Vickroy and Ray Sisson was deeply appreciated.

References

Asghari, K. and Nakutnyy, P. 2008. Experimental Results of Polymer Flooding of Heavy Oil Reservoirs. Presented at the Canadian International Petroleum Conference, Calgary, 17–19 June. PETSOC-2008-189. https://doi.org/10.2118/2008-189.

Beliveau, D. 2009. Waterflooding Viscous Oil Reservoirs. *SPE Res Eval & Eng* **12** (5): 689–701. SPE-113132-PA. https://doi.org/10.2118/113132-PA.

Clarke, A., Howe, A. M., Mitchell, J. et al. 2016. How Viscoelastic-Polymer Flooding Enhances Displacement Efficiency. *SPE J.* **21** (4): 675–687. SPE-174654-PA. https://doi.org/10.2118/174654-PA.

Craig, F. F. 1971. *The Reservoir Engineering Aspects of Waterflooding*, Vol. 3, 45–75. Richardson, Texas: Monograph Series, Society of Petroleum Engineers.

de Loubens, R., Vaillant, G., Regaieg, M. et al. 2017. Numerical Modeling of Unstable Water Floods and Tertiary Polymer Floods Into Highly Viscous Oils. Presented at the SPE Reservoir Simulation Conference, Montgomery, Texas, 20–22 February. SPE-182638-MS. https://doi.org/10.2118/182638-MS.

Delamaide, E., Let, K. M. S., Bhoendie, K. et al. 2016. Interpretation of the Performance Results of a Polymer Flood Pilot in the Tambaredjo Oil Field, Suriname. Presented at the SPE Annual Technical Conference and Exhibition, Dubai, 26–28 September. SPE-181499-MS. https://doi.org/10.2118/181499-MS.

Delamaide, E., Zaitoun, A., Renard, G. et al. 2014. Pelican Lake Field: First Successful Application of Polymer Flooding in a Heavy-Oil Reservoir. *SPE Res Eval & Eng* **17** (3): 340–354. SPE-165234-PA. https://doi.org/10.2118/165234-PA.

Doorwar, S. and Mohanty, K. K. 2017. Viscous-Fingering Function for Unstable Immiscible Flows. *SPE J.* **22** (1): 19–31. SPE-173290-PA. https://doi.org/10.2118/173290-PA.

Erincik, M. Z., Qi, P., Balhoff, M. T. et al. 2017. New Method to Reduce Residual Oil Saturation by Polymer Flooding. Presented at the SPE Annual Technical Conference and Exhibition, San Antonio, Texas, 9–11 October. SPE-187230-MS. https://doi.org/10.2118/187230-MS.

Fabbri, C., Cottin, C., Jimenez, J. et al. 2014. Secondary and Tertiary Polymer Flooding in Extra-Heavy Oil: Reservoir Conditions Measurements—Performance Comparison. Presented at the International Petroleum Technology Conference, Doha, 20–22 January. IPTC-17703-MS. https://doi.org/10.2523/IPTC-17703-MS.

Green, D. W. and Willhite, G. P. 1998. *Enhanced Oil Recovery*, Vol. 6, 103. Richardson, Texas: Textbook Series, Society of Petroleum Engineers.

Guo, H. 2017. How to Select Polymer Molecular Weight and Concentration to Avoid Blocking in Polymer Flooding? Presented at the SPE Symposium: Production Enhancement and Cost Optimisation, Kuala Lumpur, 7–8 November. SPE-189255-MS. https://doi.org/10.2118/189255-MS

Huh, C. and Pope, G. A. 2008. Residual Oil Saturation From Polymer Floods: Laboratory Measurements and Theoretical Interpretation. Presented at the SPE Improved Oil Recovery Symposium, Tulsa, 19–23 April. SPE-113417-MS. https://doi.org/10.2118/113417-MS.

Johnson, E. F., Bossler, D. P., and Bossler, V. O. N. 1959. Calculation of Relative Permeability From Displacement Experiments. SPE-1023-G.

Jones, S. C. and Roszelle, W. O. 1978. Graphical Techniques for Determining Relative Permeability From Displacement Experiments. *J Pet Technol* **30** (5): 807–817. SPE-6045-PA. https://doi.org/10.2118/6045-PA.

Koh, H., Lee, V. B., and Pope, G. A. 2017. Experimental Investigation of the Effect of Polymers on Residual Oil Saturation. *SPE J.* **23** (1): 1–17. SPE-179683-PA. https://doi.org/10.2118/179683-PA.

Kumar, M., Hoang, V. T., Satik, C. et al. 2008. High-Mobility-Ratio Waterflood Performance Prediction: Challenges and New Insights. *SPE Res Eval & Eng* **11** (1): 186–196. SPE-97671-PA. https://doi.org/10.2118/97671-PA.

Levitt, D., Jouenne, S., Bondino, I. et al. 2013. Polymer Flooding of Heavy Oil Under Adverse Mobility Conditions. Presented at the SPE Enhanced Oil Recovery Conference, Kuala Lumpur, 2–4 July. SPE-165267-MS. https://doi.org/10.2118/165267-MS.

Liu, J., Adegbesan, K. O., and Bai, J. 2012. Suffield Area, Alberta, Canada—Caen Polymer Flood Pilot Project. Presented at the SPE Heavy Oil Conference Canada, Calgary, 12–14 June. SPE-157796-MS. https://doi.org/10.2118/157796-MS.

Luo, H., Mohanty, K. K., and Delshad, M. 2017a. Modeling and Upscaling Unstable Water and Polymer Floods: Dynamic Characterization of the Effective Viscous Fingering. *SPE Res Eval & Eng* **20** (4): 779–794. SPE-179648-PA. https://doi.org/10.2118/179648-PA.

Luo, H., Delshad, M., Zhao, B. et al. 2017b. A Fractional Flow Theory for Unstable Immiscible Floods. Presented at the SPE Canada Heavy Oil Technical Conference, Calgary, 15–16 February. SPE-184996-MS. https://doi.org/10.2118/184996-MS.

Mai, A. and Kantzas, A. 2010. Mechanisms of Heavy Oil Recovery by Low Rate Waterflooding. *J Can Pet Technol* **49** (1): 44–50. SPE-134247-PA. https://doi.org/10.2118/134247-PA.

Maini, B. 1998. Is It Futile to Measure Relative Permeability for Heavy Oil Reservoirs? *J Can Pet Technol* **37** (4): 56–62. PETSOC-98-04-06. https://doi.org/10.2118/98-04-06.

Manichand, R. N. and Seright, R. 2014. Field vs. Laboratory Polymer Retention Values for a Polymer Flood in the Tambaredjo Field. *SPE Res Eval & Eng*. **17** (3): 314–325. SPE-169027-PA. https://doi.org/10.2118/169027-PA.

Manichand, R. N., Moe Soe Let, K. P., Gil, L. et al. 2013. Effective Propagation of HPAM Solutions Through the Tambaredjo Reservoir During a Polymer Flood. *SPE Prod & Oper* **28** (4): 358–368. SPE-164121-PA. https://doi.org/10.2118/164121-PA.

Moe Soe Let, K. P., Manichand, R. N., and Seright, R. S. 2012. Polymer Flooding a ~500-cp Oil. Presented at the SPE Improved Oil Recovery Symposium, Tulsa, 14–18 April 2012. SPE-154567-MS. https://doi.org/10.2118/154567-MS.

Odeh, A. S. 1959. Effect of Viscosity Ratio on Relative Permeability (includes associated paper 1496-G). SPE-1189-G.

Peters, E. J. and Flock, D. L. 1981. The Onset of Instability During Two-Phase Immiscible Displacement in Porous Media. *SPE J.* **21** (2): 249–258. SPE-8371-PA. https://doi.org/10.2118/8371-PA.

Reichenbach-Klinke, R., Stavland, A., Strand, D. et al. 2016. Can Associative Polymers Reduce the Residual Oil Saturation? Presented at the SPE EOR Conference at Oil and Gas West Asia, Muscat, Oman, 21–23 March. SPE-179801-MS. https://doi.org/10.2118/179801-MS.

Richardson, J. G. 1957. The Calculation of Waterflood Recovery From Steady-State Relative Permeability Data. *J Pet Technol* **9** (5): 64–66. SPE-759-G. https://doi.org/10.2118/759-G.

Saboorian-Jooybari, H., Dejam, M., and Chen, Z. 2015. Half-Century of Heavy Oil Polymer Flooding From Laboratory Corefloods to Pilot Tests and Field Applications. Presented at the SPE Canada Heavy Oil Technical Conference, Calgary, 9–11 June. SPE-174402-MS. https://doi.org/10.2118/174402-MS.

Sandberg, C. R., Gournay, L. S., and Sippel, R. F. 1958. The Effect of Fluid-Flow Rate and Viscosity on Laboratory Determinations of Oil-Water Relative Permeabilities. SPE-709-G.

Seright, R. 2010. Potential for Polymer Flooding Viscous Oils. *SPE Res Eval & Eng* **13** (3): 730–740. SPE-129899-PA. https://doi.org/10.2118/129899-PA.

Seright, R. S. 1988. Placement of Gels to Modify Injection Profiles. Presented at the SPE Enhanced Oil Recovery Symposium, Tulsa, 16–21 April. SPE-17332-MS. https://doi.org/10.2118/17332-MS.

Seright, R. S. 2017. How Much Polymer Should Be Injected During a Polymer Flood? Review of Previous and Current Practices. *SPE J*. **22** (1): 1–18. SPE-179543-PA. https://doi.org/10.2118/179543-PA.

Seright, R. S. and Liang, J. 1995. A Comparison of Different Types of Blocking Agents. Presented at the SPE European Formation Damage Control Conference, The Hague, 15–16 May. SPE-30120-MS. https://doi.org/10.2118/30120-MS.

Seright, R. S. and Martin, F. D. 1993. Impact of Gelation pH, Rock Permeability, and Lithology on the Performance of a Monomer-Based Gel. *SPE Res Eng* **8** (1): 43–50. SPE-20999-PA. https://doi.org/10.2118/20999-PA.

Seright, R. S., Fan, T., Wavrick, K. et al. 2011. New Insights Into Polymer Rheology in Porous Media. *SPE J*. **16** (1): 35–42. SPE-129200-PA. https://doi.org/10.2118/129200-PA.

Seright, R. S., Prodanovic, M., and Lindquist, W. B. 2006. X-Ray Computed Microtomography Studies of Fluid Partitioning in Drainage and Imbibition Before and After Gel Placement: Disproportionate Permeability Reduction. *SPE J*. **11** (2): 159–170. SPE-89393-PA. https://doi.org/10.2118/89393-PA.

Seright, R., Seheult, M., and Talashek, T. 2009. Injectivity Characteristics of EOR Polymers. *SPE Res Eval & Eng* **12** (5): 783–792. SPE-115142-PA. https://doi.org/10.2118/115142-PA.

Skauge, T., Vik, B. F., Ormehaug, P. A. et al. 2014. Polymer Flood at Adverse Mobility Ratio in 2D Flow by X-Ray Visualization. Presented at the SPE EOR Conference at Oil and Gas West Asia, Muscat, Oman, 31 March–2 April. SPE-169740-MS. https://doi.org/10.2118/169740-MS.

Sorbie, K. S. and Seright, R. S. 1992. Gel Placement in Heterogeneous Systems With Crossflow. Presented at the SPE/DOE Enhanced Oil Recovery Symposium, Tulsa, 22–24 April. SPE-24192-MS. https://doi.org/10.2118/24192-MS.

Urbissinova, T. S., Trivedi, J., and Kuru, E. 2010. Effect of Elasticity During Viscoelastic Polymer Flooding: A Possible Mechanism of Increasing the Sweep Efficiency. *J Can Pet Technol* **49** (12): 49–56. SPE-133471-PA. https://doi.org/10.2118/133471-PA

Vermolen, E. C. M., van Haasterecht, M. J. T., and Masalmeh, S. K. 2014. A Systematic Study of the Polymer Visco-Elastic Effect on Residual Oil Saturation by Coreflooding. Presented at the SPE EOR Conference at Oil and Gas West Asia, Muscat, Oman, 31 March–2 April. SPE-169681-MS. https://doi.org/10.2118/169681-MS.

Vittoratos, E. and Kovscek, A. 2017. Doctrines and Realities in Reservoir Engineering. Presented at the SPE Western Regional Meeting. Bakersfield, California, 23–27 April. SPE-185633-MS. https://doi.org/10.2118/185633-MS.

Wang, D., Cheng, J., Yang, Q. et al. 2000. Viscous-Elastic Polymer Can Increase Microscale Displacement Efficiency in Cores. Presented at the SPE Annual Technical Conference and Exhibition, Dallas, 1–4 October. SPE-63227-MS. https://doi.org/10.2118/63227-MS.

Wang, D., Xia, H., Liu, Z. et al. 2001a. Study of the Mechanism of Polymer Solution With Visco-Elastic Behavior Increasing Microscopic Oil Displacement Efficiency and the Forming of Steady "Oil Thread" Flow Channels. Presented at the SPE Asia Pacific Oil and Gas Conference and Exhibition, Jakarta, 17–19 April. SPE-68723-MS. https://doi.org/10.2118/68723-MS.

Wang, D., Cheng, J., Xia, H. et al. 2001b. Viscous-Elastic Fluids Can Mobilize Oil Remaining After Water-Flood by Force Parallel to the Oil-Water Interface. Presented at the SPE Asia Pacific Improved Oil Recovery Conference, Kuala Lumpur, 8–9 October. SPE-72123-MS. https://doi.org/10.2118/72123-MS.

Wang, D., Seright, R. S., Moe Soe Let, K. P. et al. 2017. Compaction and Dilation Effects on Polymer Flood Performance. Presented at SPE Europec featured at 79th EAGE Annual Conference and Exhibition, Paris, 12–15 June 2017. SPE-185851-MS. https://doi.org/10.2118/185851-MS.

Wang, D., Seright, R. S., Shao, Z. et al. 2008. Key Aspects of Project Design for Polymer Flooding at the Daqing Oilfield. *SPE Res Eval & Eng* **11** (6): 1117–1124. SPE-109682-PA. https://doi.org/10.2118/109682-PA.

Wang, D., Wang, G., and Xia, H. 2011. Large Scale High Visco-Elastic Fluid Flooding in the Field Achieves High Recoveries. Presented at the SPE Enhanced Oil Recovery Conference, Kuala Lumpur, 19–21 July. SPE-144294-MS. https://doi.org/10.2118/144294-MS.

Wang, D., Xia, H., Yang, S. et al. 2010. The Influence of Visco-Elasticity on Micro Forces and Displacement Efficiency in Pores, Cores and in the Field. Presented at the SPE EOR Conference at Oil and Gas West Asia, Muscat, Oman, 11–13 April. SPE-127453-MS. https://doi.org/10.2118/127453-MS.

Wang, J. and Dong, M. 2007. A Laboratory Study of Polymer Flooding for Improving Heavy Oil Recovery. Presented at the Canadian International Petroleum Conference, Calgary, 12–14 June. PETSOC-2007-178. https://doi.org/10.2118/2007-178.

Wang, J., Dong, M., and Asghari, K. 2006. Effect of Oil Viscosity on Heavy Oil-Water Relative Permeability Curves. Presented at the SPE/DOE Symposium on Improved Oil Recovery, Tulsa, 22–26 April. SPE-99763-MS. https://doi.org/10.2118/99763-MS.

Wassmuth, F. R., Green, K., Arnold, W. et al. 2009. Polymer Flood Application to Improve Heavy Oil Recovery at East Bodo. *J Can Pet Technol* **48** (2): 55–61. PETSOC-09-02-55. https://doi.org/10.2118/09-02-55.

Willhite, G. P. 1986. *Waterflooding*, Vol. 3, 21–110. Richardson, Texas: Textbook Series, Society of Petroleum Engineers.

SI Metric Conversion Factors

cp × 1.0*	E−03 = Pa·s
ft × 3.048*	E−01 = m
In. × 2.54*	E+00 = cm
md × 9.869 233	E−04 = μm^2
psi × 6.894 757	E+00 = kPa

*Conversion factor is exact.

Randy S. Seright is a senior engineer at the Petroleum Recovery Research Center of New Mexico Institute of Mining and Technology, where he has worked the past 30 years. He holds a PhD degree in chemical engineering from the University of Wisconsin, Madison.

Dongmei Wang is an assistant professor in the Harold Hamm School of Geology and Geological Engineering at the University of North Dakota. Her current research interests are enhanced oil recovery using surfactant imbibition from shale and other tight resources, as well as polymer flooding of heavy oil. Wang worked for Petrochina from 1987 to 2009 and established the document/procedure manual for the design of polymer floods throughout China. She is a member of SPE and the American Association of Petroleum Geologists and currently serves as an officer in the SPE Williston Section. Wang received SPE Outstanding Technical Editor awards in 2015, 2016, and 2017 for *SPE Journal*.

Nolan Lerner has been the vice president of development with Cona Resources Limited (formerly Northern Blizzard Incorporated) since January 2017, and also has been the team lead for the Cactus Lake asset since 2014. Before joining Cona Resources Limited in 2013, he held several positions at Penn West Exploration Limited, most recently as development team lead for the Carbonates Business Unit. Lerner previously was an exploitation engineer with a focus on conventional-waterflood management, and held positions at Talisman Energy Incorporated and Encana Corporation. He is a professional engineer and holds a bachelor's degree in industrial systems engineering from the University of Regina, Canada. Lerner is an active member of SPE and the Association of Professional Engineers and Geoscientists of Alberta.

Anh Nguyen is a senior development engineer at Cona Resources Limited. Her current interests are understanding reservoir heterogeneity and the pattern-configuration effect on recovery in heavy-oil polymer flooding at the Cactus Lake Basal Mannville Bakken Pool. Nguyen previously worked at Tundra Oil and Gas Limited, Pengrowth Energy Corporation, Enerplus Resource Corporation, Husky Energy Limited, and Wascana Energy Incorporated in various capacities, such as reservoir, process, and development engineer and team leader. She holds a bachelor's degree in chemical engineering from the University of Saskatchewan, Canada, and a management certificate from the University of Calgary. Nguyen is an active member of SPE and the Association of Professional Engineers and Geoscientists of Alberta.

Jason Sabid is an enhanced-oil-recovery development specialist at Cona Resources Limited in Calgary, where he has worked for the past 5 years in the Cactus Lake Field. Sabid holds a bachelor's degree in chemistry from the University of Alberta.

Ron Tochor is an area team lead at Cona Resources Limited and a professional engineer. He has more than 20 years of experience developing heavy-oil reservoirs in the Western Canadian Sedimentary Basin. Tochor holds a bachelor's degree in mechanical engineering from the University of Saskatchewan.